J Mater Sci (2007) 42:7934–7938
DOI 10.1007/s10853-007-1521-1

# Optimization of the Al–Cr–Zn system at 460 °C

**Richard Fourmentin · Marie-Noëlle Avettand-Fènoël · Guy Reumont · Pierre Perrot**

Received: 13 July 2006 / Accepted: 16 January 2007 / Published online: 1 June 2007
© Springer Science+Business Media, LLC 2007

**Abstract** The Al–Cr–Zn ternary system is assessed by the CALPHAD method. The solution phases are modelled using the Redlich–Kister formalism. The ternary intermetallic compounds are described by using the sublattice model. The main intermetallic compound $\tau_1$, of the Al–Cr–Zn system, was treated as $\delta_1$-$FeZn_9$ solid phase in accordance with its isotype structure. A comparison with experimental phase diagram is also presented.

## Introduction

The galvanizing process has an essential commercial importance in the production of a wide variety of corrosion resistant steel products, especially for the automotive industry. Small amounts of aluminium are added to the Zn bath for better control of the Zn–Fe reaction. Because of the use of submerged equipment in stainless steel, the bath may also contain small amounts of chromium.

The assessment of the quaternary Fe–Zn–Al–Cr diagram, essential for the understanding of the formation of both coating and dross during galvanizing, requires the study of three ternary diagrams sharing the zinc corner namely: Fe–Zn–Al [1], Fe–Zn–Cr [2], and Al–Cr–Zn. As this last diagram has not been investigated, a set of experiments was carried out in the Al–Cr–Zn system at 460 °C [3] in order to build a database for the critical assessment of this ternary system.

The thermodynamic description of the Al–Cr–Zn system at 460 °C used the CALPHAD method. In these calculations, thermodynamic properties of the alloyed system were studied with thermodynamic models for the Gibbs energy of the individual phases. The thermodynamic parameters involved in the models were assessed from measured experimental thermodynamic information and phase. For the intermetallic compounds a sublattice model was used to take account of atomic substitutions. The liquid solution phase was modelled using the Redlich–Kister formalism.

A complete assessment of the ternary system led to a better understanding of the formation of intermetallic compounds in the coating and the dross formation inside the galvanizing bath. In this case, local equilibria were explained by the equilibria between different solid phases in the ternary system.

Finally the assessed diagram was compared with the experimental diagram.

## Thermodynamic models

The isobar (with a pressure P of 101 325 Pa) optimizations and calculations of the ternary phase diagram Al–Cr–Zn at 460 °C have been carried out by the Parrot module of Thermo-Calc [4]. The optimized condensed phases of the Al–Cr–Zn system presented in this work were based on:

- the Gibbs energies of the pure elements proposed by Dinsdale [5] and available in the SGTE SSOL database;

R. Fourmentin · M.-N. Avettand-Fènoël · G. Reumont (✉) · P. Perrot
LMPGM, UMR CNRS 8517, Université de Lille I, Villeneuve d'Ascq, France
e-mail: guy.reumont@univ-lille1.fr

M.-N. Avettand-Fènoël
e-mail: Marie-Noelle.Avettand-Fenoel@univ-lille1.fr

P. Perrot
e-mail: Pierre.Perrot@univ-lille1.fr

- the binary Cr–Zn diagram assessed by Reumont et al. [6];
- the binary Al–Cr diagram assessed by Dupin et al. [7].

Isobar thermodynamic models

*Unary phases*

At a given temperature the Gibbs energy function $^{\circ}G^{\varphi}_{i}(T) = G^{\varphi}_{i}(T)–H^{SER}_{i}$ for the element i (i = Al, Cr, Zn) in the phase $\varphi$[$\varphi$ = liquid, body-centered cubic (bcc), hexagonal close-packed (hcp), face-centered cubic (fcc)] is described by an equation of the form :

$$^{0}G^{\Phi}_{i}(T) = a + bT + cT\ln T + dT^{2} + eT^{3} + fT^{-1} + hT^{-9}$$

where $H^{SER}_{i}$ is the molar enthalpy of the element i at 298.15 K in its element reference (SER) state (fcc for Al, bcc for Cr and hcp for Zn). Then, the Gibbs energy of element i in its SER state is denoted by *GHSERi* i.e.:

$$GHSERAL = G^{fcc}_{Al}(T) - H^{SER}_{Al}$$

$$GHSERCR = G^{bcc}_{Cr}(T) - H^{SER}_{Cr}$$

$$GHSERZN = G^{hcp}_{Zn}(T) - H^{SER}_{Zn}$$

In the present work, the Gibbs energy functions are taken from the SGTE compilation of Dinsdale [5].

*Solution phases*

In the Al–Cr–Zn system, the solid and liquid solutions are described by their Gibbs energies which are given by the following expression:

$$^{0}G^{\Phi}_{m}(T) = G^{\Phi}_{m}(T) - x_{Al}H^{SER}_{Al} - x_{Cr}H^{SER}_{Cr} - x_{Zn}H^{SER}_{Zn}$$

$$\begin{aligned} ^{0}G^{\Phi}_{m}(T) =& x_{Al}{}^{0}G^{\Phi}_{Al} + x_{Cr}{}^{0}G^{\Phi}_{Cr} + x_{Zn}{}^{0}G^{\Phi}_{Zn} + RT(x_{Al}\ln x_{Al} \\ &+ x_{Cr}\ln x_{Cr} + x_{Zn}\ln x_{Zn}) + {}^{XS}G^{\Phi}_{m}(T) \end{aligned}$$

where $^{XS}G^{\varphi}_{m}(T)$ is the excess Gibbs energy, expressed by a Redlich–Kister polynomial :

$$\begin{aligned} {}^{XS}G^{\Phi}_{m}(T) =& x_{Al}x_{Cr}\sum_{v=0}^{n}L^{v}_{Al,Cr}(x_{Al}-x_{Cr})^{v} \\ &+ x_{Cr}x_{Zn}\sum_{v=0}^{n}L^{v}_{Cr,Zn}(x_{Cr}-x_{Zn})^{v} \\ &+ x_{Al}x_{Zn}\sum_{v=0}^{n}L^{v}_{Al,Zn}(x_{Zn}-x_{Al})^{v} + L_{AlCrZn}x_{Al}x_{Cr}x_{Zn} \end{aligned}$$

where $L^{v}_{i,j}$ is the binary interaction parameter between i and j, which can be either Al, Cr, or Zn and $L_{AlCrZn}$ is the ternary interaction parameter between Al, Cr, and Zn.

*Stoichiometric compounds*

The Gibbs energy per mole formula unit $i_m j_p$ is expressed as following:

$$^{0}G^{i_m i_v}_{m}(T) = G^{i_m j_v}_{m}(T) - mH^{SER}_{i} - pH^{SER}_{j}$$

$$^{0}G^{i_m j_v}_{m}(T) = mGHSERi + pGHSERj + \Delta_f G^{i_m j_v}$$

where $\Delta_f G^{i_m j_p}$ represents the Gibbs energy of formation per mole of formula unit $i_m j_p$:

$$\Delta_f G^{i_m j_p} = \Delta_f H^{i_m j_p} - T\Delta_f S^{i_m j_p}$$

Due to the lack of experimental measurements, it was assumed that Neumann–Kopp's rule was applied to the heat capacity of the compounds. Hence, $\Delta_f H^{i_m j_p}$ and $\Delta_f S^{i_m j_p}$ were considered as independent of the temperature. According to the extension of intermetallics in the ternary system, the sublattice model was used in order to justify the substitution between Al, Cr, and Zn atoms in the structure of the compounds.

## Experimental information

Many experiments [3] have been carried out in the Al–Cr–Zn system at 460 °C in order to optimize the phase diagram of the Al–Cr–Zn system at 460 °C through the Parrot module.

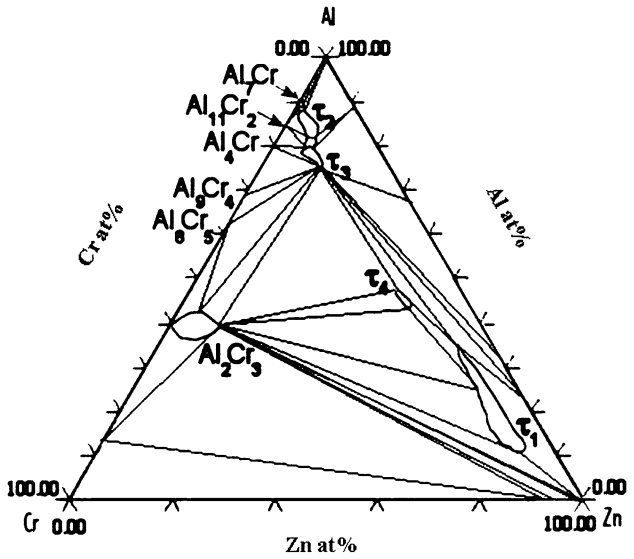


**Fig. 1** Experimental phase diagram in the Al–Cr–Zn system at 460 °C [3]

**Table 1** Assessed thermodynamical parameters

| Phase/Intermetallic compound | Description | Interaction parameter (IP) or not | Value | Reference |
|---|---|---|---|---|
| Liquid | (Al,Cr,Zn) | Cr–Zn (IP) | $L_0$ = 4528 | [6] |
| | | | $L_1$ = –1000 | |
| | | Al–Cr (IP) | $L_0$=–9552–30*T | [5, 11] |
| | | | $L_1$=2946–14*T | |
| | | | $L_2$=–12000 | |
| | | Al–Zn (IP) | $L_0$ = 10288–3.035*T | [12] |
| | | | $L_1$ =–810+0.471*T | |
| BCC-A2 | $(Al,Cr,Zn)_1(Va)_3$ | Cr–Zn (IP) | $L_0$ = 80*T | [6] |
| | | Al–Cr (IP) | $L_0$ = –55370–10*T | [5, 11] |
| | | | $L_1$ = 1830–10*T | |
| | | | $L_2$ = –8800 | |
| FCC-A1 | $(Al,Cr,Zn)_1(Va)_1$ | Al–Cr (IP) | $L_0$ = –63800–5*T | [5, 11] |
| | | | $L_1$=8000 | |
| | | | $L_2$ = –4000 | |
| | | Al–Zn (IP) | $L_0$ =–7297.48+0.47512*T | [12] |
| | | | $L_1$ = 6612.88–4.5911*T | |
| | | | $L_2$ = –3097.19 + 3.30635*T | |
| | | Cr–Zn (IP) | $L_0$ = 0 | [6] |
| HCP-A3 | $(Al,Cr,Zn)_1(Va)_{0.5}$ | Al–Zn (IP) | $L_0$ = 18820.95–8.95255*T | [12] |
| | | Cr–Zn (IP) | $L_0$ = 80*T | [6] |
| $CrZn_{13}$ | $(Al,Cr)_{0.072}(Al,Zn)_{0.928}$ | Al–Zn | $\Delta G^f_{Al-Zn} = -1250$ | [12] |
| | | Cr–Zn | $\Delta G^f_{Cr-Zn} = -595 - 0.282 \times T$ | [6] |
| | | Al,Cr:Zn (IP) | $L_0$ = –1000 | This work |
| $\tau_1$ | $(Al,Cr)_{0.125}(Al,Zn)_{0.295}(Zn)_{0.58}$ | Cr–Zn | $\Delta G^f_{Cr-Zn} = -400$ | [6] |
| | | Al–Cr–Zn | $\Delta G^f_{Al-Cr-Zn} = -9000$ | This work |
| $CrZn_{17}$ | $(Al,Cr)_{0.0556}(Zn)_{0.9444}$ | Cr–Zn | $\Delta G^f_{Cr-Zn} = -565 - 0.382 \times T$ | [6] |
| | | Al–Zn | $\Delta G^f_{Al-Zn} = -300$ | [12] |
| | | Al,Cr:Zn (IP) | $L_0$ = –1500 | This work |
| $Al_7Cr$ | $(Al)_{0.75}(Cr)_{0.1333}(Al,Zn)_{0.1167}$ | Cr–Al | $\Delta G^f_{Cr-Al} = -13389 + 0.479 \times T$ | [5, 11] |
| | | Cr–Al–Zn | $\Delta G^f_{Cr-Al-Zn} = -15000$ | This work |
| $Al_2Cr_3$ | $(Al)_{0.4}(Cr)_{0.5}(Cr,Zn)_{0.1}$ | Cr–Al | $\Delta G^f_{Cr-Al} = -19500$ | [5, 11] |
| | | Cr–Al–Zn | $\Delta G^f_{Cr-Al-Zn} = -18000$ | This work |
| $Al_4Cr$ | $(Al)_{0.8}(Cr)_{0.2}$ | Cr–Al | $\Delta G^f_{Cr-Al} = -17154 + 0.25 \times T$ | [5, 11] |
| $Al_8Cr_5$ | $(Al)_{0.6}(Cr)_{0.4}$ | Cr–Al | $\Delta G^f_{Cr-Al} = -15062 - 8.496 \times T$ | [5, 11] |
| $Al_9Cr_4$ | $(Al)_{0.692}(Cr)_{0.308}$ | Cr–Al | $\Delta G^f_{Cr-Al} = -12907 - 7 \times T$ | [5, 11] |
| $Al_9Cr_4$-L | $(Al)_{0.692}(Cr)_{0.308}$ | Cr–Al | $\Delta G^f_{Cr-Al} = -15900 - 5.5 \times T$ | [5, 11] |
| $AlCr_2$ | $(Al)_{0.333}(Cr)_{0.667}$ | Cr–Al | $\Delta G^f_{Cr-Al} = -10878 - 8.299 \times T$ | [5, 11] |
| $\tau_4$ | $(Al,Zn)_{0.48}(Cr)_{0.1207}(Zn)_{0.3993}$ | Al–Cr–Zn | $\Delta G^f_{Al-Cr--Zn} = -300$ | This work |
| | | Cr–Zn | $\Delta G^f_{Cr-Zn} = -400$ | [6] |

Pure chromium bars were dipped in Al–Cr–Zn baths; Physical Vapour Deposition (PVD) of zinc was performed on Al–Cr alloys; and chromium was added progressively to Al–Zn baths [3]. The different phases were analysed by Energy Dispersive Spectroscopy (EDS) for solid phases, Inductive Coupled Plasma (ICP) for the liquid phase, and X-Ray Diffraction (XRD) to determine the crystallographic structures. These analyses revealed new solid ternary phases:$\tau_1$,$\tau_2$,$\tau_3$,$\tau_4$, and $Al_2Cr_3$ (Fig. 1). This later phase did not appear in the Al–Cr phase diagram at 460 °C, but it shows the particularity to be stabilized with a small zinc amount (< 1 wt.%) in the Al–Cr–Zn system at 460 °C. The solubility of zinc can reach 10 wt.% in $Al_2Cr_3$ (Fig. 1).

For an increasing Al content, the liquid phase was in equilibrium, with the solid phases: fcc-Al, $\tau_3$,$\tau_1$, $Al_2Cr_3$, and $CrZn_{17}$. According to this phase diagram, the

intermetallic compound $\tau_1$ was the main phase in equilibrium with the liquid phase. XRD investigations on these intermetallic compounds showed that $\tau_1$ had the same microstructure as the $\delta_1 - FeZn_9$ solid phase [3].

For aluminium contents typical of galvanizing bath ($0.15 <$ wt.% Al $< 0.20$), the liquid was in equilibrium with $\tau_1$ and the zinc-enriched $Al_2Cr_3$ compounds. Through ICP analysis, the experimental invariant knee point $Liquid + \tau_1 + Al_2Cr_3$ was estimated as: 0.11 wt.% Al and 0.139 wt.% Cr.

## Assessment procedure

The first step consisted in optimizing Al–Cr, Al–Zn and Cr–Zn binary systems. The thermodynamic data of the Al–Cr system were given by [7]. The data of the Al–Zn system have been provided by the literature [8]. The description of the binary Cr–Zn system was given by [2] where the enthalpy of formation of the intermetallic compounds was estimated using Miedema's method [9] and their entropy of formation was fitted through experimental values.

The second step was to optimize new parameters (sublattice model) which were introduced in order to take into account the solubility of ternary intermetallics. The new experimental ternary intermetallics were modeled in order to limit their domain to a segment (Table 1). As the intermetallic compound $\tau_1$ was identified by XRD as $\delta_1 - FeZn_9$ solid phase[3], $\tau_1$ was described as $\delta_1$-$FeZn_9$ [2] (this thermodynamic and structural description allowed to introduce this compound in the quaternary Fe–Al–Cr–Zn system where $\tau_1$ and $\delta_1$-$FeZn_9$ are the same phase [10]). In the experimental description of the Al–Cr–Zn system (Fig. 1), for the Al composition range of interest for the galvanizing processes (i.e., between 0.10 and 0.20 wt.% Al), it was shown that compounds $\tau_2$ and $\tau_3$ were not in equilibrium with the liquid phase. In addition, since these two intermetallic compounds, $\tau_2$ and $\tau_3$, were very close to the $Al_7Cr$ compound containing 10 wt.% of Zn, these three compounds were eventually combine together. Thus, for the sake of clarity, $\tau_2$ and $\tau_3$ were both labeled as $Al_7Cr$, but containing 14 at.% zinc. This simplification did not modify any equilibria in the Zn rich corner.

## Results and discussion

The thermodynamic assessment of the Al–Cr–Zn system obtained in the present work is shown in Fig. 2. The liquidus (Fig. 3) is the most important part of the diagram for galvanizing experiments. Accurate placement of the liquidus allows predicting the equilibria between zinc bath, liquid phase, and zinc coating or dross. Calculations were consistent with the experimental results (Fig. 3). These results have been obtained from industrial zinc baths containing both chromium and aluminum, where the liquid phase in equilibrium with different intermetallic compounds was analyzed by ICP. Experimentally, when two types of precipitates were observed, the composition of the liquid phase corresponded to the invariant knee point, symbolized by ∇, between the equilibria $Liquid + \tau_1$ and $Liquid + Al_2Cr_3$. The experimental knee point was found very close to the optimized knee point. The other points (○, ✧, ☆, and +) were related to industrial baths where the liquid phase was in equilibrium with $\tau_1$. These results are in accord with the optimized liquidus.

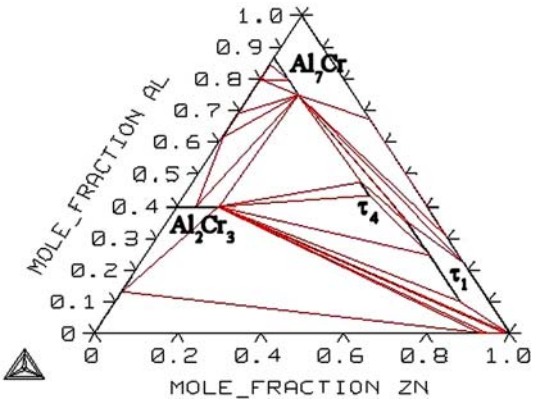


**Fig. 2** Assessed Al–Cr–Zn phase diagram at 460 °C

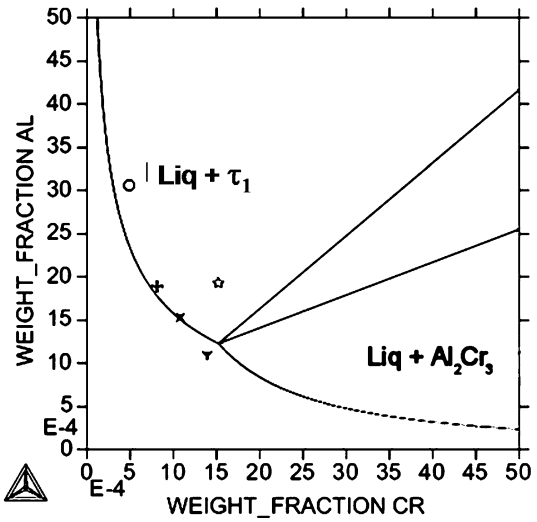


**Fig. 3** Liquidus of the Al–Cr–Zn system at 460 °C

## Conclusions

A thermodynamical evaluation of the Al–Cr–Zn system has been carried out using experimental information. The liquidus optimization was consistent with the experimental data. The database, used for the assessment of this ternary system, is now available as part of the Fe–Zn–Al–Cr database, to allow for the optimization of this quaternary system at 460 °C.

## References

1. Perrot P, Tissier JC, Dauphin JY (1992) Z Metallkd 83(11):785
2. Reumont G, Mathon M, Fourmentin R, Perrot P (2003) Z Metallkd 94:411
3. Fourmentin R, Reumont G, Perrot P, Gay B, Claessens S (2004) J Phys IV 113:65
4. Sundman B, Jansson B, Andersson JO (1985) Calphad 9:153
5. Dinsdale AT (1991) Calphad 15:317
6. Reumont G, Perrot P (2003) J Phase Equilibria 24(1):50
7. Dupin N, Ansara I, Sundman B (2001) Calphad 25(2):279
8. Murray JL (1983) Bull Alloy Phase Diag 4(1):55
9. Niessen AK, De Boer FR, Boom R, De Chatel PF, Mattens WCM, Miedema AR (1983) Calphad 7:51
10. Fourmentin R, Avettand-Fenoël MN, Reumont G, Perrot P (2005) XXXI$^{ieme}$ J.E.E.P. - Barcelona – oral communication
11. Saunders N, Rivlin VG (1987) Z Metallkde 78(11):795
12. David N, PhD thesis, Université Henri Poincaré de Nancy 1 (2001)